HARP Visible and Ultraviolet Intensity Profile and Blackbody Spectrum with 2nm Spectra

Joseph T. Emison[1] and Stephen E. Straits.[2]
Taylor University, Upland, IN, 46590
Faculty Advisors: Dr. Hank Voss and Professor Jeff Dailey

The High Altitude Research Platform (HARP) IR-UV spectrometer, Visible light intensity, and Ultraviolet types A (400-315 nm), B (315-280 nm), and C (280-100 nm) Intensity project is a high altitude balloon experiment designed to study the absorption spectrum of the gases in our atmosphere up to 35 km and to capture the solar blackbody spectrum with its absorption lines. Our sensor system includes three UV photodiodes, a visible light sensor and Ocean Optics spectrometer which are capable of measuring wavelengths over a range of 200-1025 nm at a resolution of ~1.7-2.1nm. We secured the sensor to the pod with an assembly that we designed in Solidworks and fabricated through the use of a 3D printer. In addition, we designed photocurrent amplifier for the UV photodiodes and fabricated a PC board to carry it. We individually and cross analyzed the data from each of the sensors. Documentation of the fully functional system and analysis of UV profiles may be used to reproduce the experiment for students in courses such as chemistry or astronomy without the use of the spectrometer.

Nomenclature

UVA	=	ultraviolet wavelength "a" range
UVB	=	ultraviolet wavelength "b" range
UVC	=	ultraviolet wavelength "c" range
V_{logout}	=	Log Amp Voltage output
i_{ref}	=	Reference current
i_{input}	=	Input current
R_f	=	Gain Resistor

[1] Taylor University Undergrad Student: University Nanosat Project Engineer, Engineering Physics, 236 W Reade Avenue, Upland, IN 46989.
[2] Taylor University Undergrad Student: University Nanosat Mechanical Lead Engineer, Engineering Physics, 236 W Reade Avenue, Upland, IN 46989.

I. Introduction

A. System Block Diagram

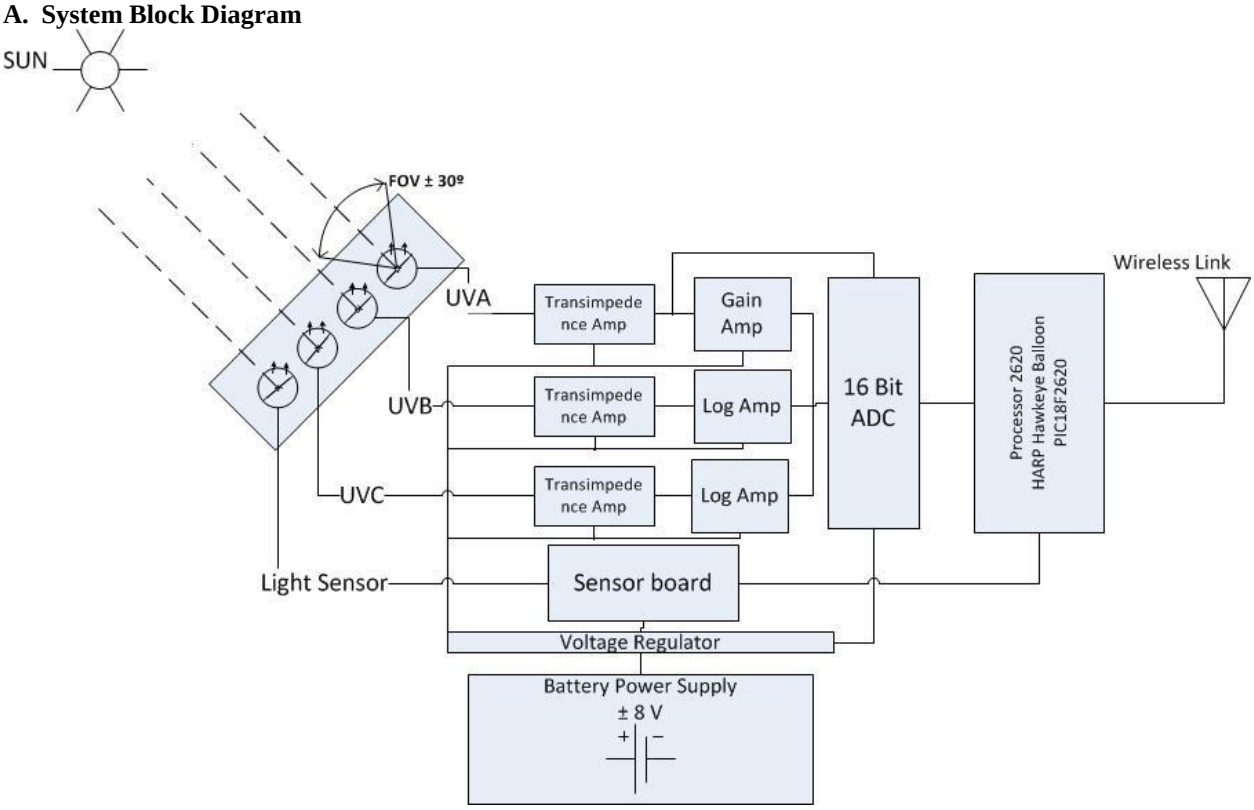

Figure 1. Pod System Block Diagram

Our system focuses on two types of wavelength in the solar irradiance spectrum, Ultraviolet and Visible light. Our goal was to study the absorption spectrum of the atmosphere in the two ranges and develop a functional circuit and mechanical system that can effectively measure each subtype in the UV range. The UV range, 100 to 400 nm, visible light range, 380 to 760nm, and the infrared range, 760nm-1mm, make up the majority of the solar radiation spectrum, which is our primary area of interest for this study. [1]

B. Definitions

1. Blackbody spectrum[2]

The electromagnetic radiation that would be radiated from an ideal black body; the distribution of energy in the radiated spectrum of a black body depends only on temperature and is determined by Plank's radiation law.

2. Absorption Spectrum[3]

The spectrum formed by electromagnetic radiation that has passed through a medium in which radiation of certain frequencies is absorbed. Generating a profile of variance and dropout, or absorption lines, in the ideally perfect radiation spectrum aids understanding of the absorption composition of our atmosphere and as well as the atmosphere of the sun.

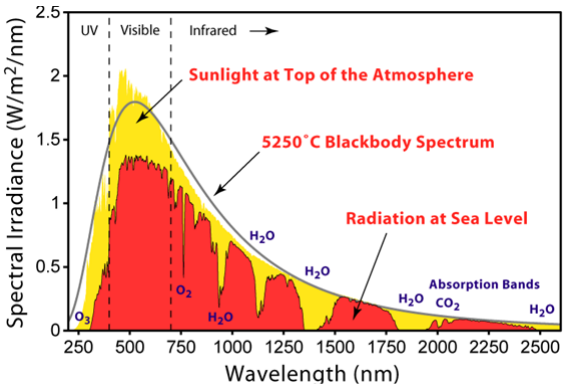

Figure 2. Solar Radiation Spectrum Graph. [4]

3. Photodiode

A photodiode is a type of semiconductor diode which operates on the principal of the photoelectric effect. Light incident on the exposed p-n junction or PIN junction of a photodiode liberates electrons which move toward the anode, or equivalently holes which move towards the cathode.

4. Ultraviolet Light[1]

Ultraviolet light has a wavelength ranging from 100-400 nanometers and is divided into three specific subtypes of UVA, UVB, and UVC with the wavelength ranges of 315-400, 280-315, and 100-280 nanometers respectively. Transmission of ultraviolet light to ground level is inversely proportional to its frequency, such that UVC has transmission roughly 0% whereas UVA has a transmission of roughly 100%. UV primarily is attenuated by interactions with the earth's ozone layer which peaks in density at roughly 20km.[5] In accordance with this principal; it logically follows that looking at relative attenuations of different UV frequencies as altitude increases may be utilized as a method of observing ozone density.

5. Field-of-View

An important parameter in analyzing the outputs of the light sensor systems is their viewing angle. The viewing angle may be defined as the angle between the pointing direction of the sensor, and the source that it is detecting. As viewing angle increases, sensitivity of the sensor decreases. By keeping track of the viewing angle of our sensors, we will be able to properly determine incident light intensity from output currents and voltages. Figure 3 to the right shows the angular sensitivity of the UV photodiodes.

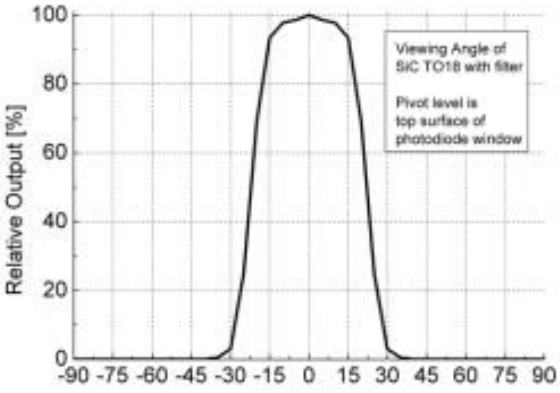

Figure 3. Viewing Angle of Photodiode SG01S-A18.[6]

6. Lux

A lux is a unit of illumination (~ brightness), equivalent to 0.0929 foot-candle and equal to the illumination produced by luminous flux of one lumen falling perpendicularly on a surface one meter squared.[7]

I. Specifications

A. Mechanical Specifications

1. *A custom assembly to secure each of the three sensor systems to the pod.*
2. *Area restriction ~ 84.95 cm^2*
3. *Standardized pod sizes (4 inch diameter)*

B. Electrical Specifications

1. *SGLux SG01s-A18 UVA Photodiode*
2. *SG01s-A18 Max spectral response (M.S.R.) 355nm*
3. *SGLux SG01s-B18 UVB Photodiode*
4. *SG01s-B18 Max spectral response 280nm*
5. *SGLux SG01s-C18 UVC Photodiode*
6. *Ocean Optics USB200-XR*
7. *Range 200-1025nm*
8. *Resolution ~1.7-2.1nm*
9. *Vernier LS-BTA visible light sensor*
10. *Range 0-150,000 Lux*
11. *Analog to Digital Converter*
12. *Range 0-5V*
13. *Resolution~ 1mV*

II. Requirements Verification Matrix

Mission Statement		
To measure, test, and analyze light spectrum in high altitude environment using sophisticated tools to observe variation in wavelengths to gain further understanding of the atmosphere with previously unexplored data.		
Number	**Missions Objectives**	**Sources**
MO-1	Generate a profile of the ultraviolet (UV) absorption spectrum of gases in our atmosphere using provided photodiodes	Taylor University (TU)
MO-2	Investigate the functionality of logarithmic amplifier technology for amplifying low currents that span multiple decades	TU
MO-3	Investigate the functionality of logarithmic amplifier technology in an environment with dynamically varying temperatures	TU
MO-4	Capture the blackbody spectrum of the sun from near space using a provided spectrometer.	TU
MO-5	Create a sustainable spectral experiment for students in general astronomy and chemistry courses	TU
MO-6	Generate a profile of visible light intensity using a provided visible light sensor	TU
Mission Design		
MD-1	The experiment will be launched on the Taylor University High Altitude Research Project (HARP)	MO-1, MO-6
MD-2	The balloon will reach a peak altitude of 35km	MO-1, MO-6
MD-3	Samples from each sensor system will be taken every 1s	MO-1, MO-2, MO-3, MO-5
Payload Requirements		
Mechanical System		
MS-1	Use 3d printer to design a mount that secures sensors to pod	MO-1, MO-5, MO-6
MS-2	externally place sensors away from pod to eliminate noise and interference for minimal error in data collection	MO-1, MO-2, MO-5, MO-6
MS-3	Secure sensors in the same relative plane and pointing angle, utilizing the zenith angle of the sun	MO-1, M0-5, MO-6
MS-4	Utilize UV sensor must have a field of view of at least ± 30°	MO-1, MO-5, MO-6
MS-5	Protection of pod's internal payload, limiting outside environment disturbances	MO-1, MO-2, MO-5, MO-6
Electrical/Sensor System		
UV Subsystem		
UV-1	SG01S-A18, SG01S-B18, SG01S-C18 photodiodes will be used to measure UVA, UVB, and UVC respectively	MO-1, MO-5
UV-2	The photocurrent amplifiers for UVB and UVC will allow an input current range over multiple decades with a maximum at ~.1nA and minimum <1pA	MSC-2, Royal Meteorological Society, Initial results a
UV-3	The photocurrent amplifier for UVA will allow input currents on the order of magnitude of 0.1uA	MSC-2, wiki, Initial results b
UV-4	Components must be rated to operate in temperatures ranging from -10C to 30C	MD-2
UV-5	A Log 114 logarithmic amplifier will be utilized as the primary amplifier for UVB and UVC photocurrent	MO-1, MO-2, MO-3, MO-5,

		UV-2
UV-6	An AD8667 electrometer amplifier will be utilized as a pre-amp to the Log 114	UV-2
UV-7	Output voltage values will be scaled, and offset if necessary, to be in the range of 5mV-5V	MSC-1, MD-1
Spectral Subsystem		
SP-1	The spectral subsystem will utilize an Ocean Optics USB2000-XR spectrometer	MO-4, MO-5
Visible Light Subsystem		
VL-1	The visible light subsystem will utilize a Vernier LS-BTA visible light sensor	MO-6
Attitude Determination Subsystem		
AD-1	An Oceanserver OS5000 Series digital compass will be utilized to determine attitude	MSC-6
AD-2	Attitude will be determined each time a measurement is taken from another sensor system	MSC-6

III. Directed Process and Design

A. Electrical Design

The electrical design consists entirely of photodiode amplifier design. At the outset of the project we were given the amplifier shown to the in Figure 4. The amplifiers used differed from the sketch in several of the resistor values because each of the photodiodes were identical.

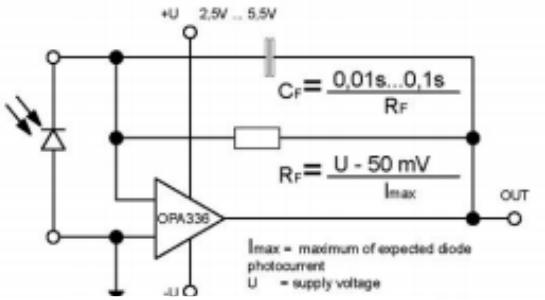

Figure 4. Photodiode Amplification Circuit.

Design changes were analyzed and considered in some detail before the first flight, but initial efforts were primarily focused on researching expected current values, which were confirmed by our the results of our first flight. The circuit in Figure 4 proved sufficient for continued use in the UVA photocurrent amplifier.
The schematic below in Figure 5 shows the design of the photodiode amplification circuit for UVB in our second flight.

The original circuit design consisted of the transimpedence amplifier described in the datasheets of the photodiodes, and a second gain stage which amplified these values. The reasoning behind having two stages is that in the case that the low gain was too low for the ADC to read, the high gain stage would be readable, and in the case that the high gain stage saturated, the low gain stage would be readable. The amplification circuit was the same for each photodiode, and the high gain value was too. Initial gain values for the UVB and UVC photodiode were found to be too low to be readable to the ADC, both in previous launches. This is described more in depth in the Flight Data Profiles and Results section below. Modification was needed in the previous op-amp gain circuits in order to boost the voltages to readable voltage values. In order to develop a circuit that provided proper amplification for the signal to be read by the ADC, we investigated the expected light incident intensity over the flight duration. In our research, we found UVA to be roughly constant, UVB would fluctuate largely over our altitude range and UVC would likely fluctuate over many orders of magnitude over small changes in altitude. When gathering more information, we made the assumption that the gain stages between those of UVA and UVC would properly amplify UVB, given the need for only approximate the intensity values. The ground intensity across the entire UV spectrum is about 32 W/m^2. With 95 percent of UVA passes to ground and majority of UVB is screened out at ground level, we estimated the peak UVA intensity would be about 5 percent higher than the total UV ground intensity. From Figure 2 of the solar radiation spectrum graph, we estimated the UVC intensity would be roughly three orders of magnitude smaller than UVA at the top of our atmosphere. At a lower altitude of 20 kilometers, the UVC intensity, as reported by Brewer and Wilson in a volume of the Royal Meteorological Society journal, is given as $1.2*10^{13}$ photons/m^2/s at a UVC wavelength of 210 nm.[6] We used the relationship E=(h)(f) to convert this to a power value of $6.815*10^{-11}$W for UVC. At lower altitudes on the order of a few thousand feet, the reported intensity value was on the order of $1.0*10^8$ photons/m^2/s, which means that the incident power would be orders of magnitude smaller. Conversely, at peak altitude, the diagram of Ozone density versus altitude graph indicates that UVC intensity would be approaching that of UVA and UVB, which represents a change by orders of magnitude. The UVC power at 20

kilometers would induce a current on the order of Pico-amps (as calculated by the multiplying the power by the peak sensitivity of the photodiode). The datasheet of the photodiode indicates that for a current this small, the resistance in the transimpedence amplifier would need to be on the order of billions of ohms. This unrealistic resistance with the large changes in UVC over small changes in altitude would result in extreme readings that would peak and minimize out of range. Furthermore, it was difficult confirm the expected values for UVC at various altitudes.
An initial solution was to use the UVA transimpedence amplifier for each photodiode followed by multiple gain stages by orders of magnitude afterwards, because only the UVA amplifier had a realistic resistance value 29 mega ohms. With the UVA transimpedence amplifier, we calculated an output voltage on the order of millivolts. This initial solution adds one gain stage to UVA, 3 gain stages for UVB, and 5 gain stages for UVC. Finding this solution to be more complex than necessary, we simplified this design using a mux to add in resistors parallel to the resistor R_f in the gain stage, where R_f alone would give the greatest possible gain. The mux could be controlled through simple code from the pod. Though simple, the solution neglected to address several factors. The risk of saturation is a major setback with the given solution. There was a distinct possibility that the initial estimates for intensities could be incorrect and if there were any unexpected results of the experiment, resulting in unreadable data. Professor Daily and Dr. Voss recommended that at this point to use a logarithmic amplifier in place of the transimpedence amplifier. Logarithmic amplifiers are capable of compressing the large signal ranges we expected due to attenuation. We chose the Texas Instruments LOG114 which has a range of 100pA to 10mA and a transfer function:

$$V_{logout} = (0.375)\left(\frac{8}{3}\right)\left(\log\frac{i_{ref}}{i_{input}}\right)$$

We also appended an AD8667 preamp to for current gain to shift the input rage of the combination down by a factor of 10,000 for an overall voltage output of 0V to 5V for an input current range of 1uA to 10fA respectively.

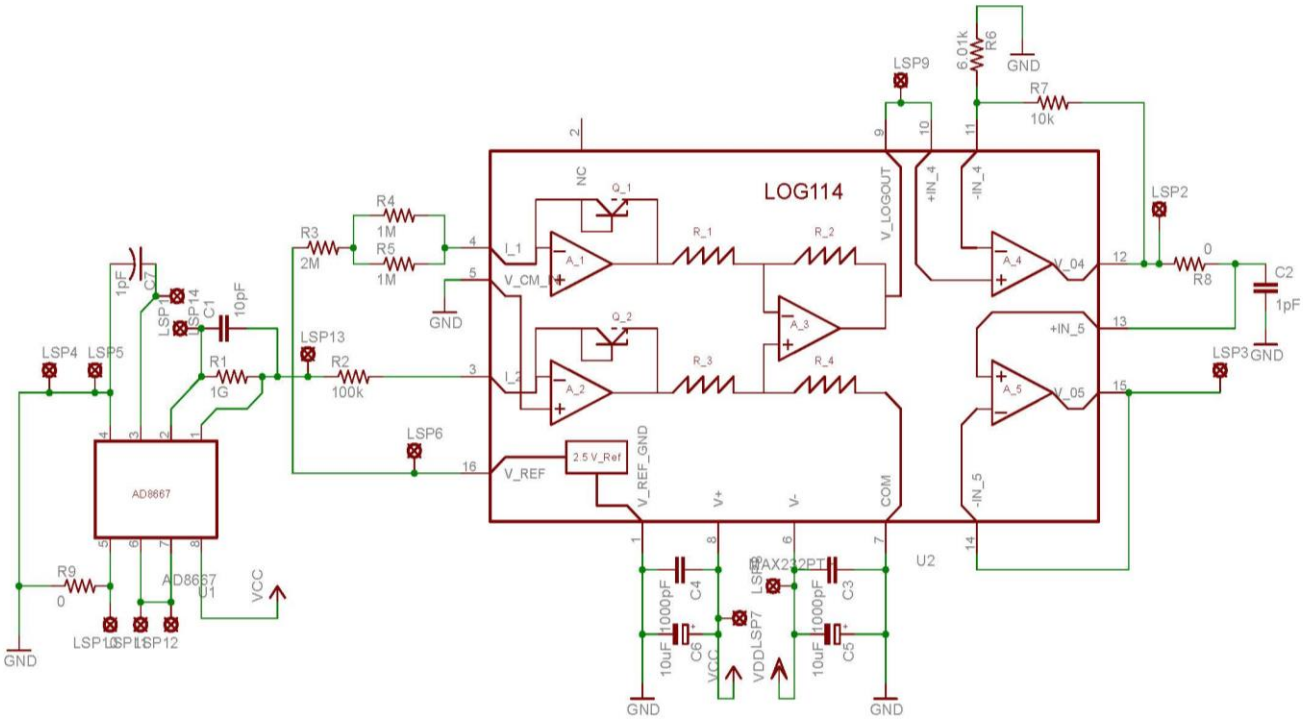

Figure 5. UVB Photodiode Amplification Circuit.

The final flight required tedious debugging of the system for the log amplifier circuit. Due to time constraints, debugging the system became implausible and we decided to forgo MO-3 and utilize the original transimpedence photocurrent amplifier design. Shown in Figure 6 to the right are the gain values for each of the amplifiers. The photodiodes utilized by each photocurrent amplifier have nearly the same MSR, and by setting each of the amplifiers with different gains we were able to experimentally find the exponential UVB profile. The experimental outputs of this amplification circuit are shown in section **V** for Flight Results.

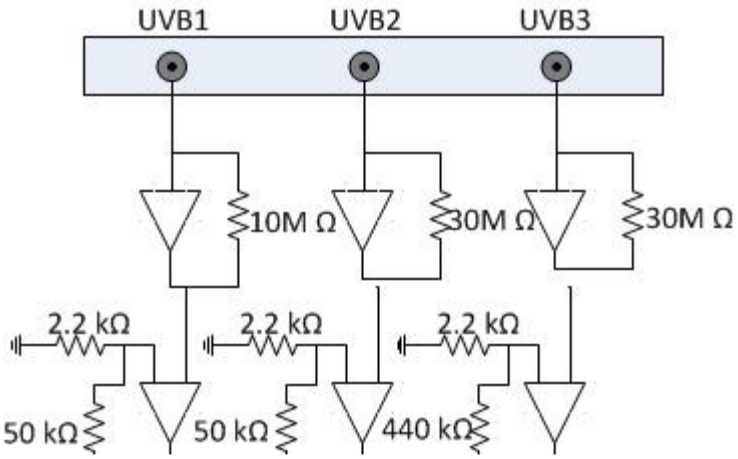

Figure 6. Block diagram for final flight of UVB photodiode amplification circuit.

B. Mechanical Design

To satisfy the requirements for the project, accurate measurements of the instrumentation dimensions were needed to fit within the pod specifications. From these requirements, we drew up different designs and created CAD models from the drawing to 3D print the mount. Our design was focused on trying to maximize the field of view, line up the sensors on the same plane pointing in the same direction, and secure the sensors to the pod to provide precision for the data gathered.

Our mechanical design was based originally off of a previous plastic mold design that held the three UV sensors straight in the same plane and screwed externally to the balloon pod. This design was functional, however did not protect the sensors from the outside elements and it did not compensate for the sun's horizon angle respective to the time of flight.

The initial re-design utilized a rectangular cube with a support securing it at the predicted horizon angle in order to minimize the error due to pointing direction. We used a slit instead of a straight cylindrical hole to provide a larger field of view in the vertical direction. The mount had five holes, each built specifically for the size of each sensor, three for the UV, one for visible light, and the last for the Ocean Optics UV-IR spectrometer. Although initially planned for, we did not include the Ocean Optic spectrometer in any of our flights.

With our first design, some modifications were required because of restriction in specs after preflight modeling. Because of the shrinking in the 3D printed plastic, the holes in the mount were too small and required manual holes to be drilled resulting in weakening the body and increasing the inaccuracy in the field of view for the sensors. Further changes were made after first flight due to failure in mounting system. Our design did not compensate for the strong g-forces applied during flight. The singular screw mount failed due to strong turbulence, which shook the mount loose in the pod. Figure 7 shows the necessary steps taken in modifying on mechanical design from the first flight to the post first flight design. One of the modifications after the first flight includes a multiple nut and bolt connection to the pod versus the singular screw attachment for our initial mount. The new design shown includes a top and bottom plate, restricting the sensors to have the same directional view and securing them in place. The first flight design greatly restricted the field of view due to the unaccounted thickness of the foam pad surrounding the pod, which is accounted for in the new design with the protrusion outside the pod. The second flight confirmed successful mechanical structure sufficient for reliable data gathering. The second flight design required a 90 degree zenith angle to capture the sun on the horizon due to the flight being a nighttime flight. The final flight was a daytime flight that compensated for the zenith angle at the time of the flight.

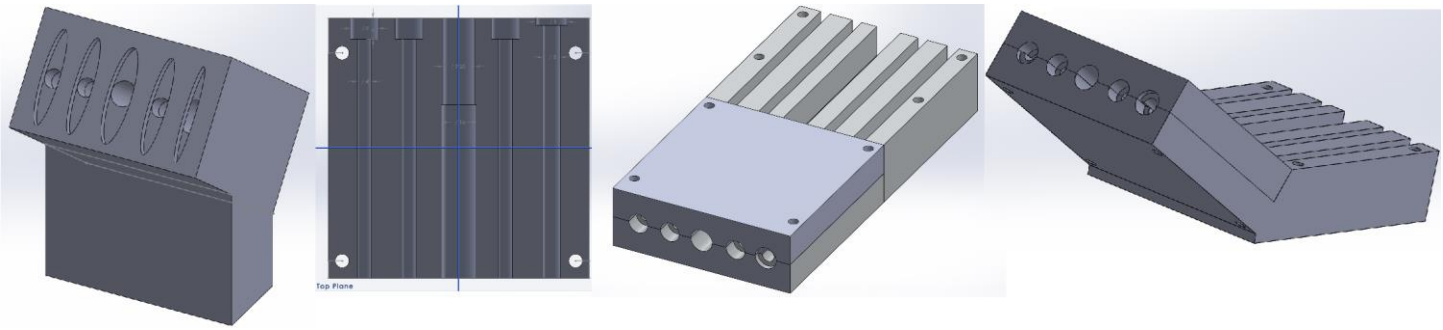

Figure 7. Sensor-mount prototype and final design. *(Left to right): First flight design, top plate for new design, second nighttime flight design, and final daytime flight design.*

IV. Testing and Prototyping

C. Flight One- March 9th, 2013

Figure 8. Balloon from Flight one.

The experiment in our first launch included the visible light sensor, UVA, and UVB photodiodes configured in transimpedence amplifier and gain amplifier circuits. Both gain values were read by the ADC and transmitted by the HARP command pod to ground. The board for the light sensor was mounted to the inside of the pod and the carrier boards for the amplifier circuits were free to move about. Figure 9 shows the sensors were wired through the mount and the pod was screwed to the baseplate of the pod.

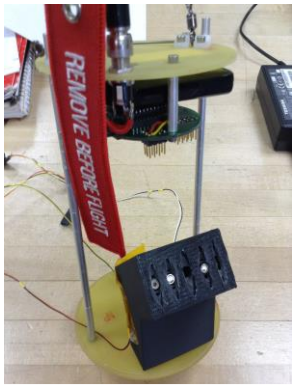

Figure 9. Assembled flight 1 pod.

D. Flight Two- April 22nd, 2013

The experiment in our second launch again included the visible light, UVA, and UVB sensors. The UVA and UVB photocurrent were amplified by the circuit shown in Figure 5**,** which we built up on a printed board. The UVC sensor was launched on a flight for a general chemistry course several days before our second launch and was not recovered in time. The dual supply power source desired for the amplification circuits were also in use, and as a result we had to run the boards on single supply. The mount was redesigned as shown to the right to account for the zenith angle of 90 degrees do the flight being at night.

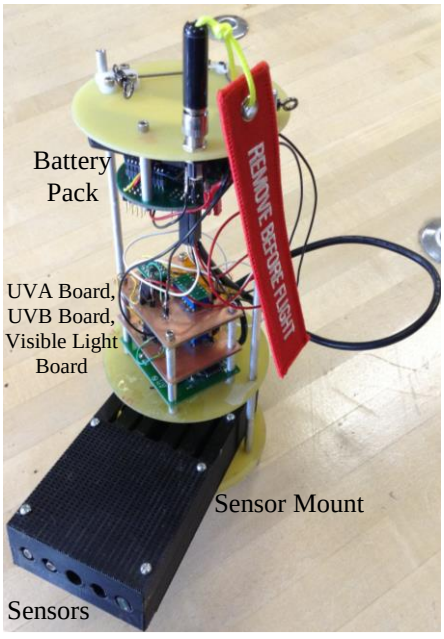

Figure 10. Assembled flight 2 pod.

E. Flight Three- June 5th, 2013

The sensor setup in the third flight utilized the dual transimpedence setup that we were given initially with new gain values which we determined from experimental data. The horizon angle on the day of the flight is approximately 32 degrees which we set as the angle of the sensor array. We flew three UVB sensors with three different gain values to reduce data losses due to saturation.

Figure 11. Assembled pod for final flight.

V. Flight Results and Preliminary Analysis

Figures 12 and 13 are altitude profiles of visible light intensity and UV photodiode amplifier output voltage respectively. The trendlines are based on the peaks of the curves, some peaks being omitted due to irregularities caused from updraft resulting in large spacing between points, low angular velocity based on the slow rate of change in the peak magnitude, and spike in intensity when traveling up above the clouds.

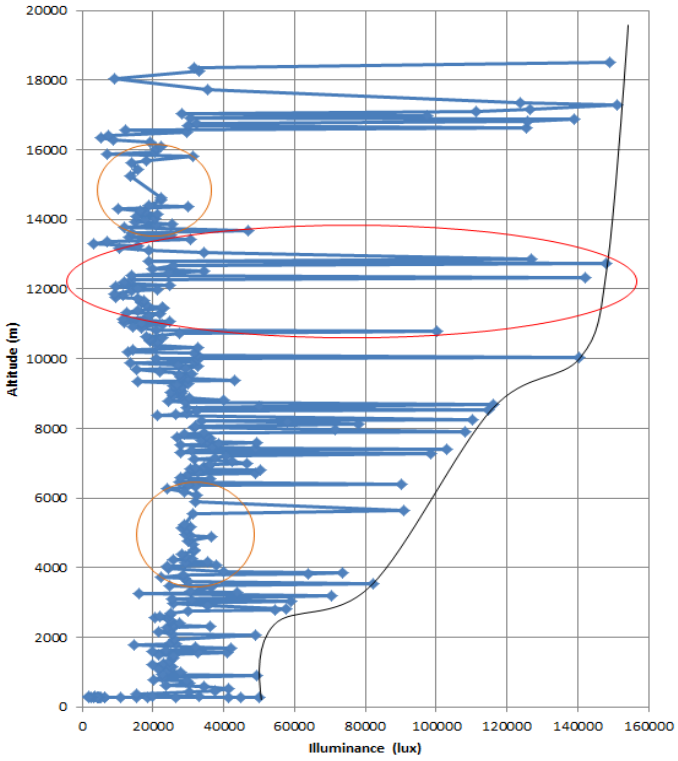

Figure 12. Flight one graph of Illuminance with respect to altitude.

The UVB intensity graph was cut off between 1-10 mV readings due to the gain being too low. The first flight did not include UVC because research indicated that with increasing altitudes its amplifier output would approach the output of the UVB amplifier and at low altitudes it would be sufficiently lower that the ADC couldn't read its output. Data from the UVA and UVB photodiodes confirmed the gain values that may be necessary for UVA, B, and C amplifiers.

We theoretically expected to observe the trendlines of the peaks to sharply increase in an exponential growth with respect to attitude resulting in a nearly vertical line in the log scale; however this result did not correspond with our theoretical expectation. The fitted curve seems to represent the low and varying angle of the sun rather than the absolute peaks at

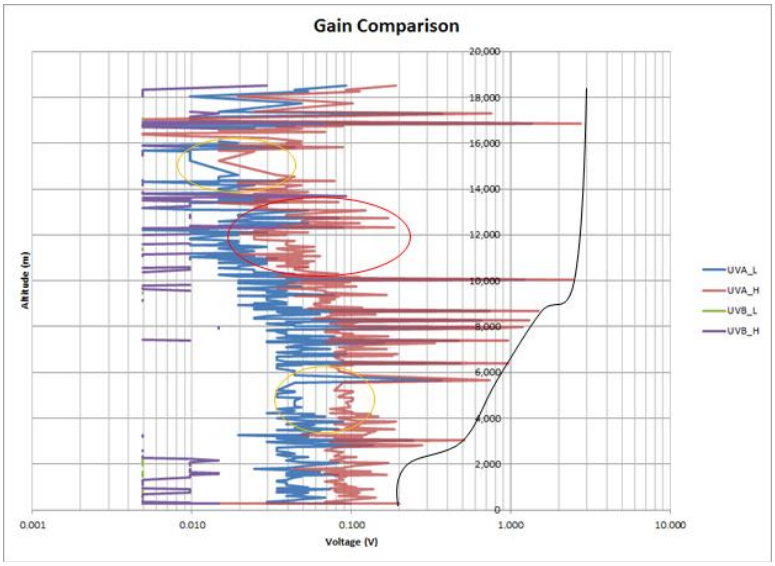

Figure 13. Log scale of flight one photodiode amplifier output voltage gain comparison, voltage with respect to altitude.

these varying heights.

From our second flight, we were unable to gather any data due to power source failure. From the initial debugging of the system, we believe that there was a short in the visible light sensor circuit. After further failure analysis of the circuit board revealed that the visible light sensor circuit board shorted out, resulting in the whole system to short and gave us no output data.

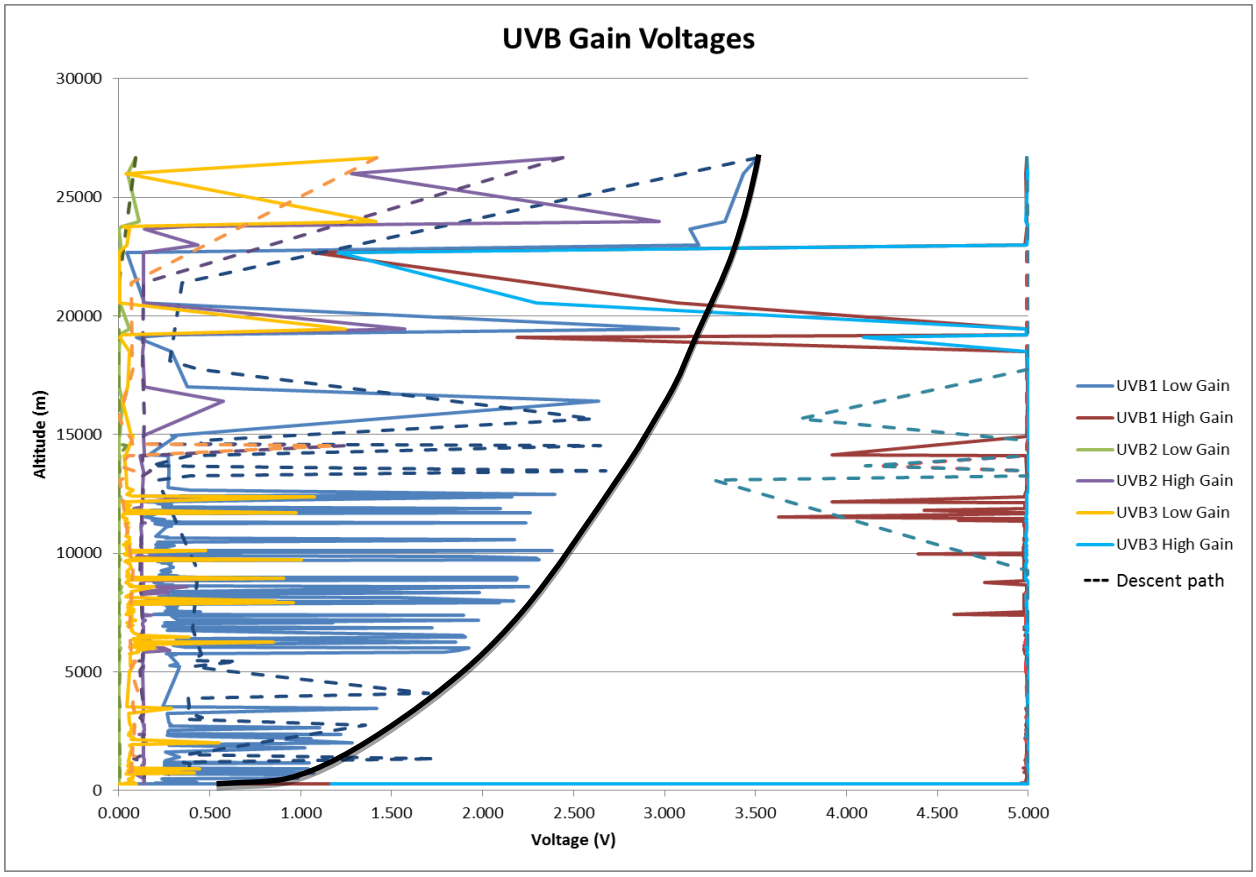

Figure 13. Final flight profile of the photodiode amplifier output voltage gain comparison, voltage with respect to altitude. *The spikes are when the sensors are looking into the sun and the minimum points when sensors are pointing away.*

In our final flight we were able to successfully gather data from our pod system, which is shown in Figure 13 above. Figure 13 shows the three different UVB photodiode amplifier low and high voltage gains with respect to the altitude. The solid lines represent outputs during ascent and the dotted lines represent outputs during descent. The output that is most preferable must not saturate, and therefore UVB1 Low gain is the best choice for analysis. We observe that the UVB1 Low Gain curve approximately fits the black exponential curve with margin included for angular sensitivity. Further analysis in the future should include a conversation directly to intensity values.

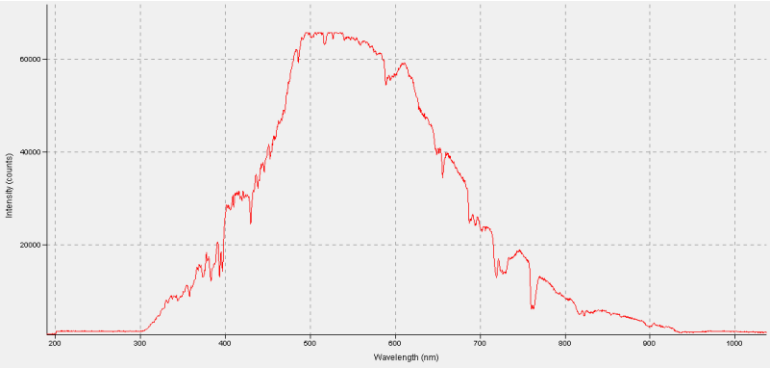

Figure 14. Ocean Optics solar ultraviolet-infrared full range intensity graph.

Using the Ocean Optics Sensor Spectrometer, we were able to capture solar radiation spectrum on the ground shown in Figure 14. The intensity appears to corner at 300nm which is longer than the wavelength of M.S.R. of the photodiodes; therefore, the spectrometer was not sufficient for comparison with the UV photodiodes. However, the spectrometer did provide useful information about the absorption spectrum of the sun, which may be analyzed by undergraduate students in future experiments.

VI. Conclusions

A. Mission Objectives Conclusion

For our project, we were able to successfully complete several of our mission objectives and requirements for each given design and payload. Looking back at the Requirement Verification Matrix in section II, we were able to completely meet MO-1, MO-2, and MO-6 and partially meet MO-3, MO-4, and MO-5. We were only able to partially meet MO-3 because we were unable to successfully run the logarithmic amplifier in the flights, however the circuit design work functionally in the bread board testing phase. We were able to capture the blackbody spectrum of the sun from the ground using the Ocean Optics spectrometer, however we were not able to capture it in near space and so MO-4 was not fully met. From this project we were able to create a sustainable experiment for undergrads; however the experiment requires some more effort in gain determination to fully meet the MO-5 requirement. For our design and payload requirements, we were able to fully meet most of the subsystem requirements; however the attitude determination subsystem was descoped due to time restraints. Future projects should include a comprehensive descope plan.

B. Documentation

The projects progress has been recorded and documented through our Spectrum Analysis Report for flight one, failure analysis reports of flight one, two, and three. Further documentation includes our published academic journal abstract, CAD modeling and the upcoming Academic High Altitude Conference.

C. Educational Experience

Through this project we have gain a greater understanding of how different sensors work. We gained experience designing and building the pod with its parts using CAD 3D modeling and printer, problem solving and failure analysis, analyzing real data, and publishing process of an academic journal.

VII. Acknowledgements

We would like to thank NSF CCLI Grant and Indiana Space Grant Consortium (INSGC) for financial support of this project. We would also like to acknowledge Dr. Voss and Prof. Dailey for providing their help in assembly and designing of the balloon pods, guidance for critical thinking, support and insight in our design process, and educational development throughout this project. Furthermore, we acknowledge Gordon Miller for his help in development and debugging of our circuit.

References

[1]"Space Environment-Process for Determining Solar Irradiances" *International Standard ISO 21348*. 2007. 9 May 2013.

[2]Princeton University "Blackbody Radiation." WordNet. Princeton University. 2010. [http://wordnetweb.princeton.edu/perl/webwn?s=blackbody%20radiation Accessed 5/9/13.]

[3]"Absorption Spectrum." *Dictionary.com Unabridged*. Random House, Inc. 9 May 2013. [http://dictionary.reference.com/browse/absorption spectrum Accessed 5/9/13.]

[4]Lund, Halvor, R. Nilsen, O. Salomatova, D. Skåre, and E. Riisem. "Solar Cells: Basic Principles of Photovoltaics." 2008. [http://org.ntnu.no/solarcells/pages/Chap.2.php Accessed 5/30/13.]

[5]"Solve II Science Information." *NASA*. Craig, Michael and Dan Chirica. 21 March 2013. [http://www.espo.nasa.gov/solveII/implement.html Accessed 5/9/13.]

[6]"SG01S-A18." *Sglux The UV Experts*. sglux, GmbH, Berlin. WEEE No. DE 76297302. 9 May 2013.

[7]"Lux." *Dictionary.com Unabridged*. Random House, Inc. 31 May 2013. [http://dictionary.reference.com/browse/lux Accessed 5/31/13.]

[8]Brewer, A.W. and A.W. Wilson. "Measurement of solar ultraviolet radiation in the stratosphere." *Quarterly Journal of the Royal Meteorological Society*, Vol. 91, Issue 390, Oct. 1965, pp.452-461.